A Common Molecular Mechanism Underlies Two Phenotypically Distinct 17p13.1 Microdeletion Syndromes

Adam Shlien,[1,2] Berivan Baskin,[3] Maria Isabel W. Achatz,[4] Dimitrios J. Stavropoulos,[3,5] Kim E. Nichols,[6] Louanne Hudgins,[7] Chantal F. Morel,[8] Margaret P. Adam,[9] Nataliya Zhukova,[1] Lianne Rotin,[1] Ana Novokmet,[10] Harriet Druker,[10] Mary Shago,[3] Peter N. Ray,[1,3,11] Pierre Hainaut,[12] and David Malkin[1,2,10,*]

DNA copy-number variations (CNVs) underlie many neuropsychiatric conditions, but they have been less studied in cancer. We report the association of a 17p13.1 CNV, childhood-onset developmental delay (DD), and cancer. Through a screen of over 4000 patients with diverse diagnoses, we identified eight probands harboring microdeletions at *TP53* (17p13.1). We used a purpose-built high-resolution array with 93.75% breakpoint accuracy to fine map these microdeletions. Four patients were found to have a common phenotype including DD, hypotonia, and hand and foot abnormalities, constituting a unique syndrome. Notably, these patients were not affected with cancer. Moreover, none of the *TP53*-deletion patients affected with cancer (n = 4) had neurocognitive impairments. DD patients have larger deletions, which encompass but do not disrupt *TP53*, whereas cancer-affected patients harbor CNVs with at least one breakpoint within *TP53*. Most 17p13.1 deletions arise by Alu-mediated nonallelic homologous recombination. Furthermore, we identify a critical genomic region associated with DD and containing six underexpressed genes. We conclude that, although they overlap, 17p13.1 CNVs are associated with distinct phenotypes depending on the position of the breakpoint with respect to *TP53*. Further, detailed characterization of breakpoints revealed a common formation signature. Future studies should consider whether other loci in the genome also give rise to phenotypically distinct disorders by means of a common mechanism, resulting in a similar formation signature.

Introduction

As the range of diseases associated with copy-number variation (CNV) expands, it has become apparent that specific CNV loci can be associated with a spectrum of unrelated conditions. For example, CNVs at 1q21.1 predispose one to schizophrenia (MIM 181500),[1,2] tetralogy of Fallot (MIM 187500),[3] cancer (including neuroblastoma [MIM 256700][4]), and a range of pediatric conditions.[5] It is unclear whether individuals harboring structural changes at these and other hotspots are predisposed to one or many diseases. High-resolution copy-number platforms, such as tiling oligonucleotide arrays, offer increased accuracy[6] and can therefore be applied to disentangle overlapping CNV-based diseases. Furthermore, characterization of CNVs at the single-base-pair level can unearth common sequence elements, which represent signatures of the various DNA repair processes that led to their formation.

Most pediatric cancers arise sporadically; however, at least 5%–10% harbor an underlying germline defect,[7] and there is an emerging link between CNVs and cancer susceptibility.[4,8,9] We have previously shown that germline *TP53* (MIM 191170) missense mutations predispose one to the autosomal-dominant cancer-susceptibility condition known as Li-Fraumeni syndrome (LFS [MIM 151623]),[10] in which an excess of CNVs across the genome are observed.[8] Here, we investigate whether 17p13.1 CNVs, which include *TP53,* are sufficient to cause LFS.

To improve our understanding of 17p13.1 CNVs, we constructed an oligonucleotide comparative genomic hybridization (CGH) array to interrogate this genomic region at ultrahigh resolution; overlapping probes covering all exons of every gene in the region, were designed to achieve 93.75% breakpoint accuracy. Using this platform, we set out to determine whether patients with 17p13.1 CNVs contain shared breakpoint sequences, critically deleted genes, or common clinical features.

Material and Methods

Sample Recruitment

Samples were collected from The Hospital for Sick Children, Stanford University Hospital, The Children's Hospital of Philadelphia, The University Health Network (Toronto), Hospital do Câncer A.C. Camargo, and Emory University. Research was approved by each center's institutional review board.

[1]Genetics & Genome Biology Program, The Hospital for Sick Children, Toronto, ON M5G1X8, Canada; [2]Department of Medical Biophysics, University of Toronto, Toronto, ON M5G1X8, Canada; [3]Division of Molecular Genetics, Department of Paediatric Laboratory Medicine, The Hospital for Sick Children, Toronto, ON M5G1X8, Canada; [4]Hospital A.C. Camargo, 01509-010 São Paulo, Brazil; [5]Department of Laboratory Medicine and Pathobiology, University of Toronto, Toronto, ON M5G1X8, Canada; [6]Division of Oncology, Children's Hospital of Philadelphia, Philadelphia, PA 19104, USA; [7]Department of Pediatrics, Division of Medical Genetics, Stanford University School of Medicine, Stanford, CA 94305, USA; [8]Department of Medicine, University Health Network, University of Toronto, Toronto, ON M5G1X8, Canada; [9]Department of Human Genetics, Emory University School of Medicine, Atlanta, GA 30033, USA; [10]Division of Hematology/Oncology, The Department of Pediatrics, University of Toronto, The Hospital for Sick Children, Toronto, ON M5G1X8, Canada; [11]Department of Molecular Genetics, The University of Toronto, Toronto, ON M5G1X8, Canada; [12]Molecular Carcinogenesis and Biomarkers Group, International Agency for Research on Cancer, 69372 Lyon, France
*Correspondence: david.malkin@sickkids.ca
DOI 10.1016/j.ajhg.2010.10.007.

TP53 Sequencing

All exons and at least 50 bp into exon-intron boundaries of *TP53* were sequenced in all available samples (7/8). No base pair sequence mutations were found.

CGH Microarray Design and Hybridization

Six of eight patients' DNA was hybridized to custom arrays. Two samples (from cancer patients) had insufficient DNA for custom array analysis, and their breakpoints were not fine mapped. We instead used multiplex ligation-dependent probe amplification (MLPA) to determine the extent of *TP53* exon deletions. Because their exact breakpoints are not known, we excluded them from statistics regarding formation signature (see below). Array CGH was performed with the use of a customized 4×44K microarray platform (Agilent Technologies, Santa Clara, CA, USA), with genomic DNA extracted from peripheral blood via standard methods. A total of 40,577 oligonucleotide probes were placed on the short arm of chromosome 17, in which an 8 Mb target region around *TP53* was covered in ultrahigh resolution. Of the 38,061 in the target region, 15,762 (41%) were designed on exons. Exonic probes were overlapping and tiled across all exons, of all alternative splice variants, for every gene. A minimum of one probe per 350 bp was placed in intronic and nongenic regions. An additional set of probes was designed to also extend our coverage to the telomere and centromere of chromosome 17p but at a reduced density (Figure S3, available online). With this array design, we hoped to capture all copy-number changes anywhere within 8 Mb of *TP53*, from small, single-exon-sized alterations (45–350 bp) to large macroscopic events, and to quickly obtain breakpoint information of copy-number changes, especially those within protein-coding regions. The lab performing array experiments was blinded to all previous results (sequencing, MLPA, quantitative PCR [qPCR], etc.). Patient and male reference DNA were labeled with Cy3-dCTP and Cy5-dCTP (PerkinElmer, Waltham, MA, USA), respectively, with the use of the BioPrime genomic labeling module (Invitrogen, Carlsbad, CA, USA) and were hybridized to the array platform, as recommended by the manufacturer's protocol (Agilent Technologies). The arrays were washed and scanned with the Agilent G2505B microarray scanner. Data analysis was performed with DNA Analytics version 4.0 (Agilent Technologies). Although this approach is capable of ascertaining both forms of copy-number change (namely deletions and duplications), only deletions were found in this cohort.

Gene-Expression Arrays and Analysis

RNA was extracted from blood via standard methods, assessed by Bioanalyzer (Agilent Technologies), and hybridized to Affymetrix Exon 1.0 microarrays (Affymetrix, Santa Clara, CA, USA). High-quality RNA was available for one individual with a large 17p13.1 deletion (encompassing *TP53*), two individuals with small 17p13.1 deletions (disrupting *TP53*), and two individuals harboring germline *TP53* missense mutations. RNA samples from three noncarrier siblings were used as controls. Gene-expression analysis was performed with the use of the Partek Genomics Suite (Partek, St. Louis, MO, USA).

Breakpoint Simulation

Custom software was developed for the simulation of CNV deletions across all autosomal chromosomes in the human genome. For each size range (from 10 Kb to 2 Mb), 10,000 simulated CNVs were assessed for intersection with Alu elements at both breakpoints.

Quantitative PCR

To obtain better size information on these deletions, we developed a high-throughput quantitative assay by using an automated liquid handling system in a 384-well plate format with 176 qPCR probes (Table S2) to target and detect the copy number of a large region of chromosome 17 (1.3 Mb). qPCR assays were performed on a Roche LightCycler by relative quantification. qPCR plates were set up with the use of a custom script and an automated liquid handling system. Primers were designed with the use of Primer3 and the human genome reference assembly (UCSC Genome Browser, version hg18). Deletion sizes were found to be larger than that reported by array CGH or MLPA and, on average, were improved by 31% with the use of this assay. The developmental delay (DD)-associated deletions were nearly 100 times larger than those involved in early-onset cancer.

Fluorescence In Situ Hybridization

Fluorescence in situ hybridization (FISH) was performed with the use of standard protocols.[11]

Parent-of-Origin Analysis

SNP genotyping was performed with Affymetrix GeneChip 250 Sty arrays or by direct sequencing. Microsatellite-marker genotyping was performed by The Center for Applied Genomics at The Hospital for Sick Children.

Breakpoint Mapping

After custom-array processing and analysis, breakpoints were mapped by first designing primers flanking the predicted breakpoints and then amplifying junction-specific fragments with the use of long-range PCR (Roche Expand Long Template PCR System). Junction fragments were subjected to sequencing. Putative breakpoints were analyzed by BLAST, BLAT, and manual inspection.

Results

Rare CNVs at *TP53* Are Associated with Cancer Predisposition or Developmental Delay

Our six diagnostic labs screened 4524 patients with diverse clinical phenotypes for DNA dosage changes via array CGH or MLPA (Table S1). Eight probands with a microdeletion at *TP53* (17p13.1), a tumor-suppressor gene that predisposes one to early-onset cancer when mutated in LFS, were identified.[10] We performed interphase and metaphase FISH, using *TP53* and 17ptel probes (Figure 1A). The interstitial deletion could be seen in all cells and was therefore not due to mosaicism.

Individuals with microdeletions at *TP53* had cancer (n = 4) or a noncancer phenotype (n = 4) comprising a spectrum of congenital anomalies (Table 1 and Figure S2) that included pervasive DD and mental retardation, speech difficulties, hypotonia, hand and foot abnormalities, and facial dysmorphisms.

Different 17p13.1 Breakpoints Are Related to Two Distinct Phenotypes

Several congenital syndromes are known to also occur in association with cancer predisposition. Such dual phenotypes are frequently caused by gene dosage mutations, either through numerical chromosomal abnormalities or

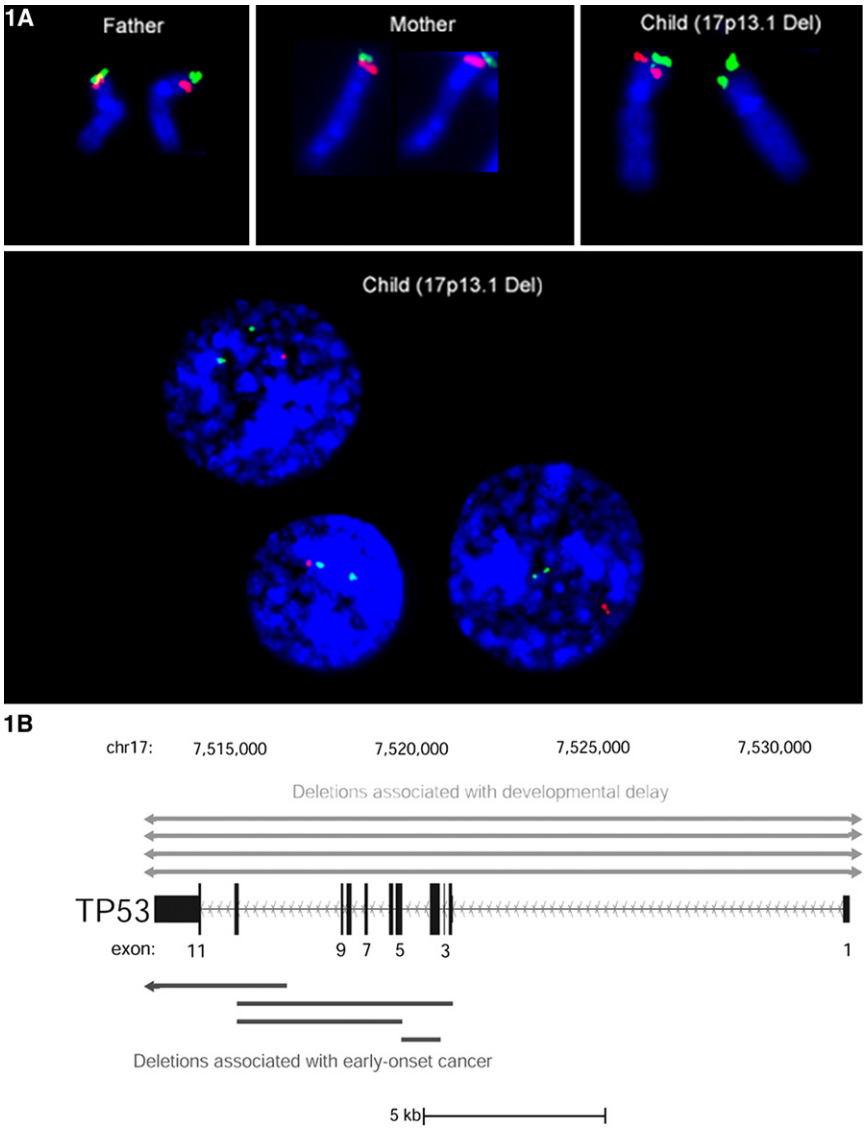

Figure 1. Discovery of a 17p13.1 CNV Leading to Two Distinct Phenotypes

(A) FISH experiments using *TP53* (red) and 17ptel (green) probes. The fluorescent signals in this representative family trio confirm a de novo hemizygous *TP53* deletion in the child's metaphase and interphase nuclei. Two hundred nuclei were scored, and no evidence of mosaicism for the CNV was observed. *TP53* microdeletions were not observed by conventional Giemsa banded karyotyping.

(B) Results of MLPA, qPCR, and clinical array revealed two isoforms of the 17p13.1 CNV. Among DD patients, the CNV includes and extends past *TP53* in the telomeric and centromeric directions (n = 4; top); Among the cancer-affected patients, the 17p13.1 CNV deletes some—but not all—of *TP53*'s exons. TP53 is transcribed off of the minus DNA strand; therefore, its introns and exons are drawn from last to first.

through specific structural changes (e.g., trisomy 21[12]). In contrast, LFS patients do not show increased rates of neurocognitive disability or any phenotype besides cancer. Consistent with this, none of the *TP53*-deletion patients affected with cancer had DD or congenital anomalies. Similarly, none of the patients with DD exhibited any neoplastic growth that might suggest an underlying susceptibility, nor did they have family histories of cancer consistent with LFS. Therefore, although they share genomic alterations at *TP53,* their distinct clinical presentations suggest that these patients fall into two nonoverlapping groups.

Next, we determined the genetic basis of this dichotomy. Our initial patient discovery was performed on two platforms, with complementary depth and breadth. Clinical array CGH provides low resolution at *TP53* but provides more information on the extent of 17p13.1 CNVs beyond *TP53*, whereas MLPA provides high resolution across *TP53*'s 11 exons but provides little information for the surrounding regions. To determine whether CNVs defined by MLPA extend beyond *TP53*, we used qPCR to determine the copy number of the genes immediately flanking *TP53* (Figure S1). Both *ATP1B2* (telomeric; MIM 182331) and *WRAP53* (centromeric; MIM 612661) were disomic in all cancer patients (mean copy numbers = 2.03 and 2.11, respectively). However, all patients with DD were hemizygously deleted for both flanking genes (mean copy numbers = 0.87 [*ATP1B2*] and 1.13 [*WRAP53*]), a significant reduction in comparison to the cancer patients ($p = 2.90 \times 10\text{-}4$ [*ATP1B2*] and $2.42 \times 10\text{-}8$ [*WRAP53*]). We also carried out MLPA experiments on all array-CGH-ascertained samples, and we found that in every DD case all 11 exons of *TP53* were contiguously deleted. In contrast, no cancer case harbored a CNV that included all 11 exons. These results demonstrate that our cohort of DD and cancer patients have overlapping but genotypically distinct CNVs at *TP53*; whereas DD-associated CNVs include all exons of *TP53* as well as flanking genes, cancer-associated CNVs are within *TP53*, causing a change in copy number to some— but not all—of its exons (Figure 1B).

17p13.1 Genomic Deletions Can Be Inherited or Arise De Novo

A review of the eight probands' pedigrees showed that families of DD patients did not have neurocognitive impairment and that the pedigrees of the four cancer patients were consistent with LFS (Figure S2). All DD

Table 1. Phenotypic Features of Four Patients with 17p13.1 CNVs and Developmental Delay

Patient ID	3026	2723	3148	3354
Sex	F	F	F	M
Age (yrs)	33.67	7.58	5.75	3.50
Inheritance	–	de novo	de novo	de novo
Parental origin	paternal	paternal	maternal	–
Cognitive	***GDD; nonverbal***; severe MR	***GDD***; ***speech apraxia***	***GDD; limited speech development***	***GDD***
Growth (percentile)	height, < 3rd; weight, < 3rd; HC, 50th	height, 25th; weight, 70th; HC, 25th	height, 10th–25th; weight, 75th–90th; HC, 97th	height, 50th–75th; weight, 50th–75th; HC, 10th–25th
Facial features	***prominent nasal bridge; high-arched palate; thin lips; high forehead;*** bilateral low-set ears; ***earlobe pits; downslanting palpebral fissures; short neck*** with webbing; ***highly arched eyebrows*** that extend laterally; low hairline; left-sided mild ptosis; recessed chin; bitemporal narrowing	***upturned nasal tip; high-arched palate; thin, puckered lips; brachycephaly***	***wide nasal bridge; high-arched palate; high forehead; downslanting palpebral fissures; broad, flat epicanthal folds; small, recessed chin; downturned corners of mouth***; telecanthus; depressed nasal tip; bifid uvula; posterior hair whorl	***broad, upturned nose*** with small nares; ***upswept ear lobules with earlobe pits; short neck*** with no webbing; unusually ***arched eyebrows; epicanthal folds; small, recessed chin; downturned corners of mouth;*** mildly upslanting palpebral fissures; short columella with prominent ala nasi
MSK features	***ligamentous laxity; bilateral elbow contractures***	***extra flexion creases (calves, arms)***; mild pectus deformity	***ligamentous laxity; contractures of the elbow and knees; dimpling at*** ankles ***elbows, and knees; sacral crease***; bilat vagus; deformity of ankles	***asymmetric crease with deep sacral dimple***; 13 pairs of ribs; mild spine curvature; partial sacralization of lower lumbar spine
Cardiovascular	VSD	PDA (self-resolved)	normal	no echocardiogram
Ocular	***strabismus***	***strabismus***; legally blind; right eye hamartoma (CHRPE-like lesion); iris hypoplasia; astigmatism; decreased lacrimation	***bilateral alternating exotropia***; myopia	lateral vision difficulty and difficulty tracking (11 mo of age)
Bone marrow	hemolytic anemia of infancy (self-resolved); pure red cell aplasia (onset age 15 yrs)	N/A	N/A	N/A
Neurological	***hypotonia; brisk DTRs; ankle clonus; hydrocephalus***; broad-based gait; brain MRI: arrested	***hypotonia; brisk DTRs; ankle clonus;*** external ***hydrocephalus***; choreoathetoid movements; brain MRI: thinned CC, delayed myelination, tethered cord; upgoing plantar responses	***hypotonia***; brain MRI: normal	***hypotonia***; DTRs difficult to elicit
Audiology	normal	normal	decreased hearing	normal
Psychiatric	***PDD***; bipolar disorder	***PDD***	N/A	N/A
Behavioral	self-injurious; aggressive	intermittent hand-wringing and hand clapping	N/A	N/A
Hands	***thumbs proximally placed; short hands***; bilateral deep palmar creases; bilateral first-finger clinodactyly; bilateral 5th finger IP joint contracture	***left thumb proximally placed; short hands*** (3rd–25th percentile); broad thumbs	left transverse palmar crease; right "hockey stick"-shaped crease	normal

Table 1. *Continued*

Patient ID	3026	2723	3148	3354
Feet	***short feet; big toe abnormally long and narrow bilaterally***; bilateral deep plantar creases; flat feet; bilateral shortened fourth toe	***small feet*** (< 5th percentile); ***big toe large and broad bilaterally; pollicization of big toes***	normal	***shortened feet with broad big toes***
GU	normal	neurogenic bladder; ovarian cysts; resolved renal cysts	normal	shawl scrotum
Skin	normal	dermoid cyst above left eye; compound melanocytic nevus; epithelioid cell type of scalp	normal	sacral Mongolian spot
Nipples	normal	***bilateral inverted*** supernumerary ***nipple***	N/A	***bilateral inverted nipples***
Other	failure to thrive and ***feeding difficulties; sleep disturbances***; hypothyroidism and iron overload secondary to blood transfusions every 3–4 weeks	***feeding difficulties; sleep disturbances; GERD***; chronic constipation; hypogammaglobinemia	***feeding difficulties; GERD***; benign paroxysmal torticollis	N/A

Bolded and italicized text indicates features shared by more than one patient. Abbreviations are as follows: HC, head circumference; CC, corpus callosum; CHRPE, congenital hypertrophy of the retinal pigment epithelium; DTR, deep tendon reflexes; GDD, global developmental delay; GERD, gastro-esophageal reflux disease; IP, interphalangeal; MR, mental retardation; PDD, pervasive developmental disorder.

patients with available parental samples (n = 3) had a de novo deletion, as shown by CGH, MLPA, and FISH analysis (200 nuclei tested, with no evidence of low-level mosaicism in parents). Among the cancer patients with deletions, familial samples were available in two cases. Of these, one family's samples were sufficiently informative to establish inheritance of the deletion. No apparent parent-of-origin bias was observed for deletions in either group of our cohort.

Design of a Custom Ultrahigh-Resolution Tiling Array

Obtaining sequence-level resolution is the most definitive method of validating rearrangements,[13] because it leads to precise definitions of the CNVs' breakpoints and gene content, provides clues as to the mechanism underlying their formation,[14,15] and reveals their potential architectural complexity.[16]

We designed an ultrahigh-resolution array covering 8 Mb of chromosome 17 to get close to sequence-level resolution and to use it as a clinical diagnostic platform for identifying all possible rearrangements in future patients. The array comprises ~45,000 oligonucleotide probes spanning 4 Mb upstream and 4 Mb downstream of the *TP53* locus (7,512,444 to 7,531,588). All exons within this region are tiled, representing the entire coding sequence of 182 genes and all possible alternative transcripts (2,130 exons; Figures S3A and S3B). The precise array design and probe placement are described in Material and Methods and Figure S3.

We tested our custom array on patients whose breakpoints we had already successfully sequenced. These experiments yielded highly precise size and breakpoint information. For example, a patient with DD was found, by the 17p13.1 array, to have a contiguous genomic deletion of 923,492 bp, a difference in size of only 2183 bp (0.2%) from that established by sequencing. The 5′ and 3′ breakpoints of the deletion were 2341 bp and 153 bp away from the true breakpoints, respectively.

Alu Short Interspersed Nuclear Repeats Are Associated with Breakpoints

Using this array, we determined the size and breakpoints of the remaining samples. Using long-range PCR, we amplified junction fragments spanning putative breakpoints. Then, in cases for which high-molecular-weight DNA was available, we sequenced junction fragments and determined the breakpoint and size of the deletions. The average difference between actual CNV sizes and the arrays' predicted sizes was 6.25% (i.e., 93.75% accuracy).

By array, one patient was revealed to harbor another deletion in 17p13.1. The secondary deletion, which is also heterozygous, is 24 Kb in length and is located downstream of the primary deletion's distal breakpoint (Figure S4). In another instance, an identical deletion was found in the proband and the proband's sibling, indicating the inheritance of the same pathogenic CNV (Figure 3, patient 3332). Although asymptomatic, the sibling is now undergoing routine biochemical and radiographic surveillance for cancer.

We looked for repeat elements coinciding with CNV breakpoints. Of the 12 sequenced breakpoints, ten directly intersect with an Alu short interspersed nuclear repeat

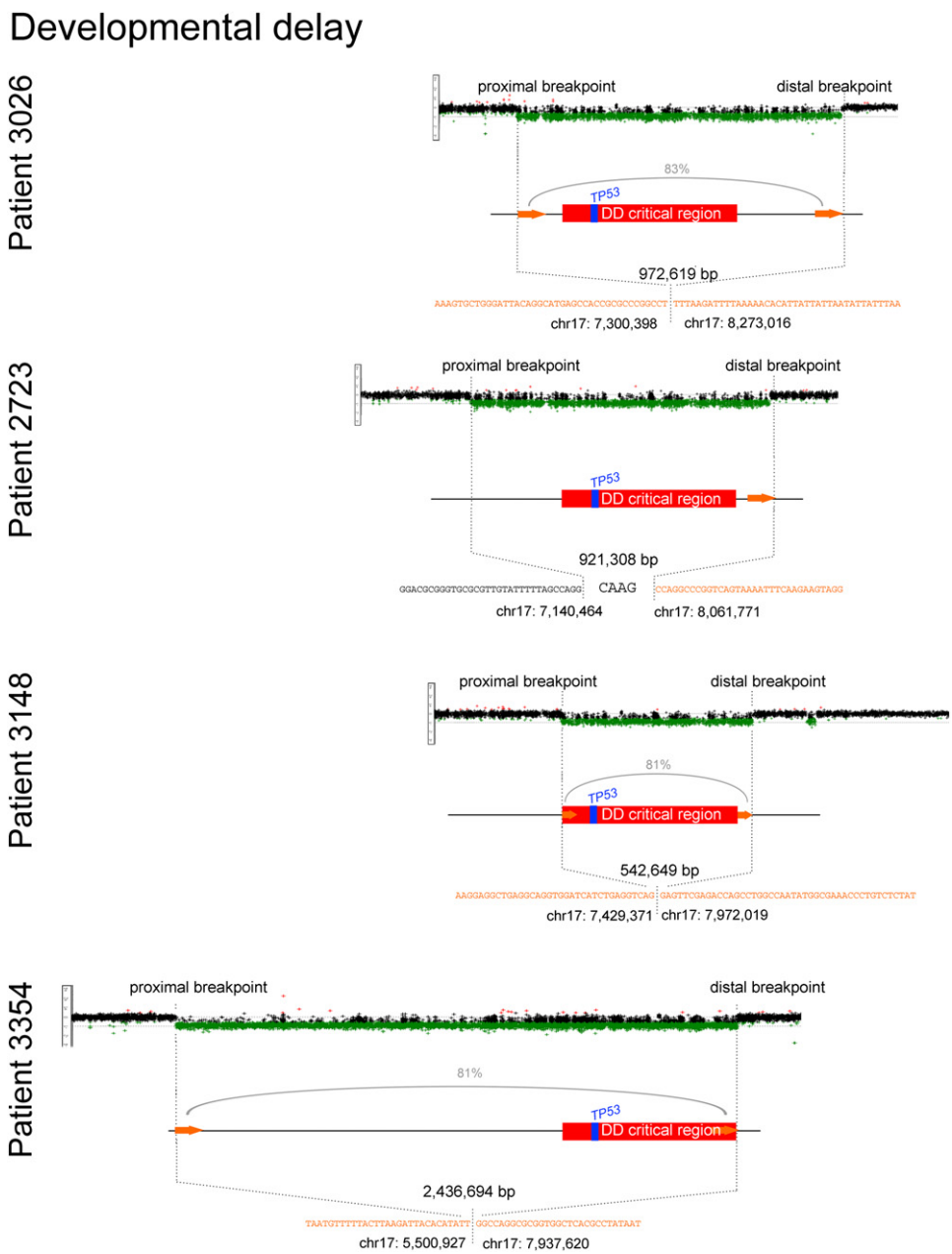

Figure 2. Breakpoint Maps, Sequence Resolution, and Inferred Mechanism of DD-Associated 17p13.1 CNVs
We developed an ultrahigh-resolution CGH array (see Figure S3) to obtain breakpoint-level information on 17p13.1 CNVs. Shown are the array results for all four DD patients. Log_2 ratios from the array are shown, each dot representing one probe and deletions indicated in green. The proximal and distal breakpoints were determined for all samples, revealing that all DD patients shared a critical region including *TP53* and 23 other genes (red). The precise breakpoint positions, their sizes, and the nucleotide sequence of the disrupted regions are shown. The presence of two Alu elements (orange arrows and orange-colored nucleotides) at the junctions is consistent with the formation of the CNV by Alu-Alu-mediated NAHR (patients 3026, 3148, and 3354). The percentage of homology between directly oriented Alus is indicated for NAHR CNVs. In one instance an NHEJ signature could be seen at the at the breakpoint sequence: Four additional base pairs incorporated at the junction (patient 2723).

element (one from the oldest AluJ family, seven from the intermediate AluS family, and two from the young AluY family).

Most 17p13.1 CNVs Arise by Alu-Mediated Nonallelic Homologous Recombination

Analysis of sequenced CNVs revealed the mechanisms by which they arose. Four of six deletions involved nonallelic homologous recombination (NAHR) between Alu elements present at both the proximal and the distal ends (Figure 2, patients 3026, 3148, 3354; Figure 3, patient 3332). The Alu elements flanking these deletions were in the same orientation and shared a moderate degree of homology (81%–84% similarity by BLAST). The remaining two patients did not exhibit extensive homologies spanning their breakpoints. Of these, one breakpoint showed

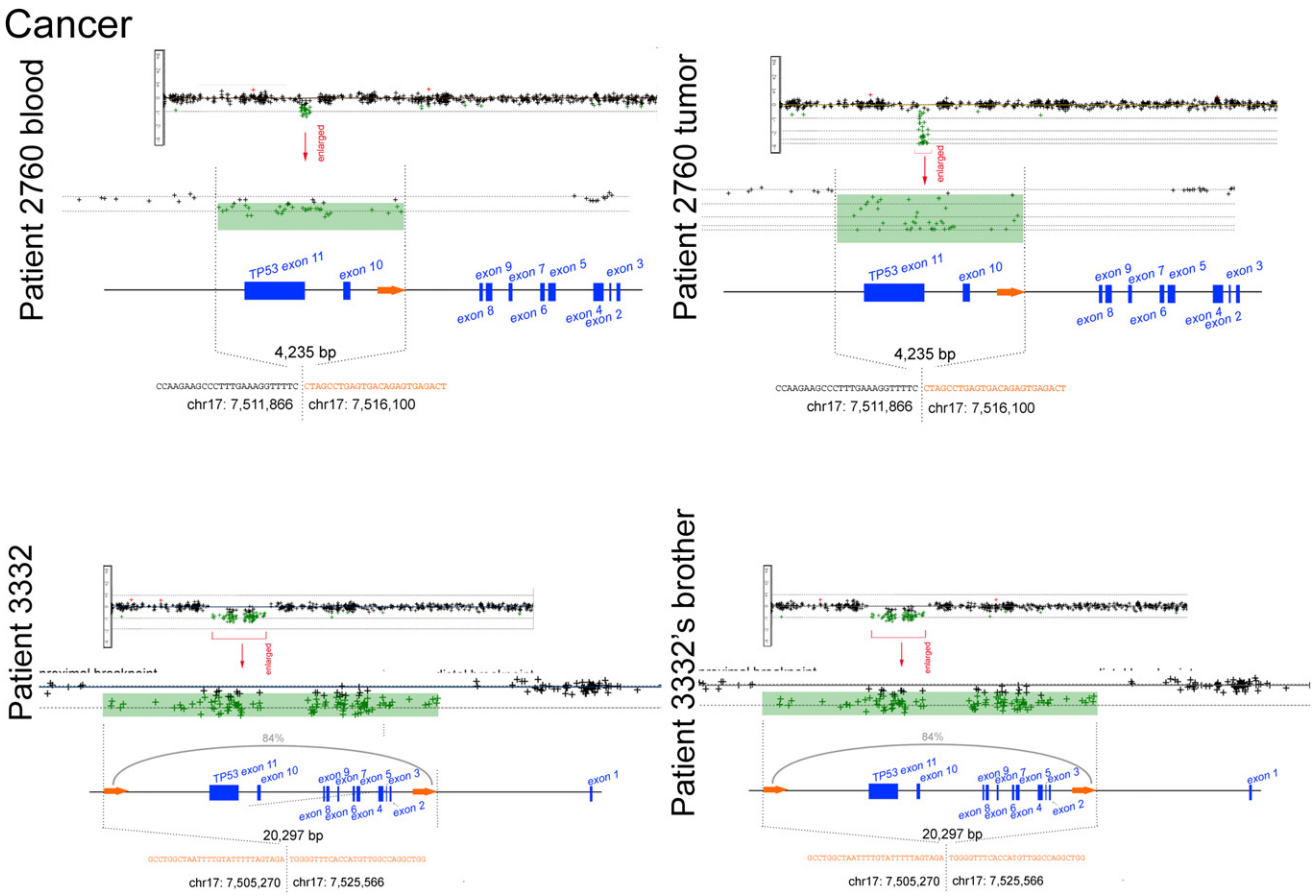

Figure 3. Breakpoint Maps, Sequence Resolution, and Inferred Mechanism of Cancer-Associated 17p13.1 CNVs
An ultrahigh-resolution CGH array (see Figure S3) was used to obtain breakpoint-level information on 17p13.1 CNVs in two cancer-affected patients. Log_2 ratios from the array are shown, each dot representing one probe and deletions indicated in green. The precise breakpoint positions, their sizes, and the nucleotide sequence of the disrupted regions are shown. The presence of two Alu elements (orange arrows and orange-colored nucleotides) at the junctions is consistent with the formation of the CNV by Alu-Alu-mediated NAHR (patient 3332 and brother). The percentage of homology between directly oriented Alus is indicated for NAHR CNVs. The proximal and distal breakpoints were always either intronic in *TP53* or intragenic, never disrupting other genes besides *TP53* or leading to gene fusions. Using high-quality DNA from one patient's frozen tumor, we observed a second deletion on the opposite allele, conforming to the classical two-hit hypothesis of tumorigenesis[42] (patient 2760). This custom array was used to test for the presence of the CNV in two asymptomatic siblings of an index case affected with cancer (patient 3332). One sibling (shown) was found to harbor the identical deletion.

a 4 bp microinsertion (CAAG), an "information scar" that is a hallmark of nonhomologous DNA end joining[17] (NHEJ; Figure 2, patient 2723).

To evaluate the significance of the observed number of Alus at 17p13.1 CNV breakpoints, we performed 10,000 permutation experiments using randomly distributed CNVs of different sizes (10 Kb to 2 Mb). In these simulations, less than 1% of breakpoints coincided with an Alu pair in the same orientation. In contrast, the majority of 17p13.1 CNVs coincide with directly oriented Alus (67%; Figure S5).

A Common Region Implicates Candidate Genes in Developmental Delay

In our study cohort, all CNVs associated with occurrence of childhood cancer were limited to the *TP53* locus, deleting between one and ten of 11 exons. Such deletions are predicted to cause protein truncation, thus interfering with the gene's tumor-suppressive activity. Indeed, in a paired tumor specimen we observed an additional copy-number alteration of the same size, thus inactivating the wild-type allele (Figure 3, patient 2760).

In contrast, in the four patients with DD we found, by fine mapping, a common deleted region (Table 2) that includes 24 genes (critical region shown in Figure 2). There are a number of candidate genes for the observed phenotypes. The four patients with DD harbored between 27 and 86 fully deleted genes. Additionally, fine mapping revealed that two DD patients carried partial deletions of genes, disrupting some but not all of their exons (Table 2).

We evaluated the effect of this 17p13.1 CNV on mRNA levels by using expression arrays (see Material and Methods). Among the genes in the minimally deleted region, the expression of *TP53* was significantly

Table 2. Deleted and Disrupted Genes in 17p13.1-Deletion Patients

Patient	Chr.	Start	End	No. of Deleted Genes	Disrupted Gene
Developmental Delay					
1	17	7,300,398	8,273,016	55	*CHRNB1*
2	17	7,140,464	8,061,771	58	–
3	17	7,429,371	7,972,019	28	*MPDU1*
4	17	5,500,927	7,937,620	86	–
Patients 1–4: Critical region	17	7,429,371	7,937,620	24	*MPDU1*
Cancer					
1	17	7,511,866	7,516,100	1	*TP53*
2	17	7,505,270	7,525,566	1	*TP53*
3	17	7,512,445	7,519,262	1	*TP53*
4	17	7,520,037	7,520,315	1	*TP53*

The four patients with DD harbored between 27 and 86 fully deleted genes and two partially deleted genes. The minimally deleted region includes 24 genes.

underexpressed in the patient affected with cancer but not in the patient with DD ($p = 6.82 \times 10^{-3}$; fold change = −1.85797; Figures 4A and 4B).

The expression of six other genes (of the 24 candidates in the region) were significantly changed in the patient with DD but not in the cancer-affected patient (Figure 3B; $p < 0.01$; fold change < -1.5 or > 1.5). Of these DD-specific genes, which are both hemizygously deleted and underexpressed in all patients, the trafficking protein particle complex 1 gene (*TRAPPC1* [MIM 610969]) is particularly intriguing. *TRAPPC1*, involved in vesicular transport from the endoplasmic reticulum to the Golgi apparatus as part of the TRAPP complex, is the most significantly changed at 17p13.1 and, of note, is also the most significantly changed gene genome-wide (Figure S6; $p = 2.90 \times 10^{-5}$; fold change = −2.34146).

Three additional DD-specific genes are noteworthy: *MPDU1* (MIM 604041), mutations of which result in congenital disorder of glycosylation type If involving severe mental and psychomotor retardation;[18] *FXR2* (MIM 605339), a homolog of the fragile X mental retardation gene, *FMRP* (MIM 309550), which itself may play a role in that disease;[19] and *EFNB3* (MIM 602297), known to be important in the development of normal locomotor behavior.[20] To determine whether the deletion unmasks a recessive mutation, we sequenced these four genes, but we did not find additional mutations.

Having found reduced *TP53* expression in the cancer-affected individual, we examined whether other *TP53* signaling-pathway members were altered. We first measured the mRNA levels of a proband from an LFS family carrying an established deleterious base pair mutation (Arg273Cys) and conducted pathway analysis. Using the well-annotated Ingenuity Pathway Analysis "Core Pathways," we noted a subtle but significant difference of genes in the *TP53* pathway in individuals with either an established mutation or an internal deletion of *TP53*, but not in those with complete deletions and DD ($p = 4.74 \times 10^{-2}$ and 3.01×10^{-2}, respectively). This shows that TP53 is aberrantly expressed in individuals affected with cancer but not in those affected with DD. Furthermore, we find that disregulated genes common to the missense- and internally-deleted-mutation carriers are associated with known molecular mechanisms of cancer ($p = 2.59 \times 10^{-3}$). Together, these data highlight gene-expression differences between individuals having large or small CNVs at 17p13.1.

Discussion

LFS is a highly penetrant susceptibility to cancer that disproportionately affects the young. Children with germline *TP53* mutations are at a 20% risk of developing cancer by 15 years of age and, over a lifetime, have a 73% to 100% risk.[21] However, the four DD patients in this report, ranging in age from 3.5 to 33.67 yrs, are not affected with cancer despite harboring complete deletions of *TP53*. Other case reports highlight an additional six patients with 17p13.1 deletions,[22–25] of whom none are affected with cancer. Although these reports support our contention that DD-associated deletions involve reduced cancer risk, it is premature to discount the possibility that these patients may have a high risk of developing cancers due to somatic *TP53* mutation, which may become manifest only at later ages.

The molecular basis for this apparent absence or reduction of cancer risk remains to be elucidated. Studies of mouse models of LFS as well as the somatic mutation spectra of *TP53* in human cancers provide evidence that tumorigenesis is accelerated when *TP53* is altered by point mutations or short insertions or deletions, rather than completely lost. In contrast, a number of nonsense mutations that predict total absence of TP53 expression are

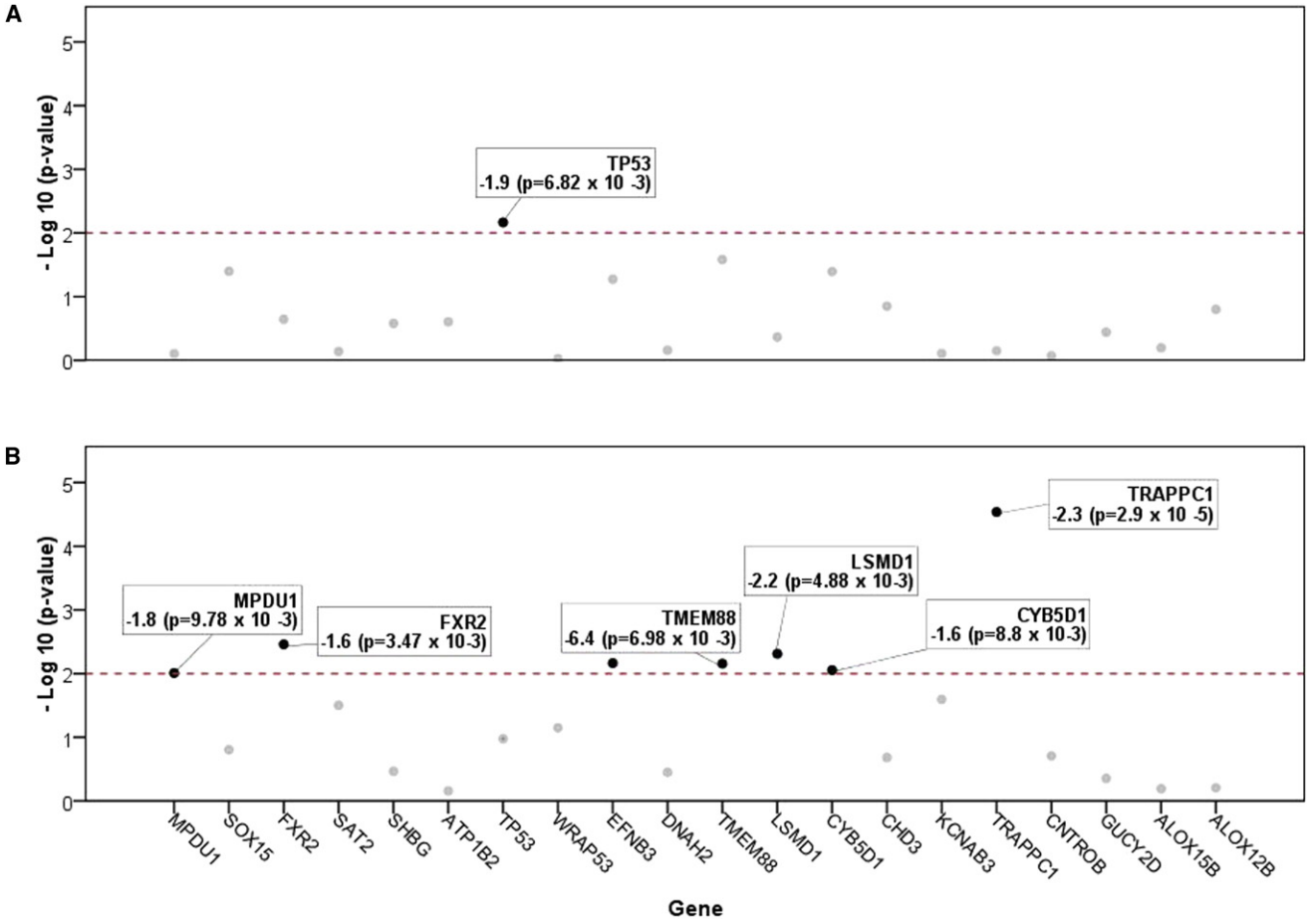

Figure 4. Gene-Expression Differences Distinguish between Cancer-Affected an DD Patients with 17p13.1 Deletions
We used Affymetrix exon arrays to look for gene-expression differences in available blood-derived RNA. We first evaluated which of the 24 genes in our critical region (commonly deleted in patients with DD) is significantly under- or overexpressed. Twenty of these 24 genes could be assayed with the array and are shown. On the *y* axis is depicted the significance of each gene's expression change relative to controls (plotted in reverse order). The red dotted line represents the p value threshold of 0.01, above which all significant changes in gene expression are highlighted (black dots).
(A) Among patients with small 17p13.1 CNV only *TP53's* expression is significantly changed ($p = 6.82 \times 10^{-3}$; fold change = −1.9).
(B) Notably, a similar analysis of RNA from a DD patient did not show *TP53* underexpression, despite the gene being fully deleted in a large 17p13.1 CNV. There are, however, six significantly changed genes (all underexpressed). As shown, these are *TRAPPC1* ($p = 2.90 \times 10^{-5}$, fold change = −2.3), *FXR2* ($p = 3.47 \times 10^{-3}$, fold change = −1.6), *LSMD1* ($p = 4.88 \times 10^{-3}$, fold change = −2.2), *KDM6B* ($p = 6.98 \times 10^{-3}$, fold change = −6.4), *CYB5D1* ($p = 8.80 \times 10^{-3}$, fold change = −1.6), and *MPDU1* ($p = 9.78 \times 10^{-3}$, fold change = −1.8). In a separate analysis (Figure S6), *TRAPPC1* was found to be the most significantly underexpressed gene in the transcriptome.

strongly associated with cancer. It should be noted that in the cancer-prone patients described here the deletions do not include exon 1 and the long intron 1. It is possible that sequences in the latter region may contribute to regulate TP53 suppressor function. In particular, the proximal region of intron 1 contains sequences encoding a natural antisense transcript of *TP53*, *WRAP53*, which regulates endogenous *TP53* mRNA by targeting the 5′ untranslated region of *TP53* mRNA.[26] The exact role of this sequence in predisposition to cancer deserves further study. Notwithstanding this caveat, we show here that mRNA expression levels of *TP53* and *TP53*-dependent genes are altered in patients with partial, but not complete, deletions—consistent with mutant *TP53*-initiated tumorigenesis in the former group but not in the latter. In contrast, the neurocognitive-delay phenotype is characterized by the dysregulation of a different set of six genes at 17p13.1 and, in particular, *TRAPPC1*, which is also the most significantly underexpressed gene in the transcriptome.

Our data support a model in which partial deletions lead to the expression of a truncated protein, rather than the complete absence of it due to nonsense-mediated decay. Truncated and wild-type protein (from the opposite allele) would oligomerize to form a defective TP53 tetramer, leading to a dominant-negative or gain-of-function effect similar to that observed with certain missense mutations, resulting in inhibition of wild-type TP53 function.[27,28] We and others have previously shown that *TP53* alterations, whether somatic or inherited, are more commonly

missense than nonsense or truncating mutations.[29] Tumors will frequently accumulate dysfunctional TP53 that is structurally intact. As such, tumors derive a greater advantage from retaining dysfunctional TP53 instead of eliminating it entirely. Likewise, in this study we demonstrate that partial deletions lead to a stronger cancer-predisposition phenotype than full-length deletions of *TP53*. Like their somatic equivalents, these "first hits" to *TP53* involve the expression of dysfunctional TP53, which as a transcription factor leads to the aberrant expression of a number of targets. We go on to show that more TP53 targets are dysfunctional in this group than in persons harboring large and complete *TP53* deletions. In light of the existing literature, we view these results as aberrant transcription of TP53 targets resulting from qualitative difference in the expressed TP53 protein, not necessarily because of a quantitative difference in its abundance. Among its many targets, TP53 also regulates its own mRNA. This feedback loop is made possible by the direct binding of TP53 and its mRNA, which forms a stable-stem loop structure.[30] Additionally, TP53 induces genes that regulate its mRNA, such as Wig-1, which stabilizes TP53 mRNA.[31] Wrap53 also stabilizes TP53 mRNA, but instead of being induced by TP53, it lies immediately proximal to it on chromosome 17p13.1.[26] Mutant TP53 disrupts many of these autoregulatory loops through aberrant binding or transactivaion. In this study, we show that this disruption, which leads to reduced TP53 mRNA (Figure 4A), is associated with partial but not large *TP53*-deletion mutants.

We designed a tiling array to determine accurate breakpoints of CNVs at 17p13.1, the locus that we also show to be responsible for a unique congenital syndrome. By achieving base pair resolution, we gained insight into the genomic basis of this dysmorphology syndrome, including the precise determination of deletion length and gene content, the definition of a critical region, and the recognition of a shared mechanism of CNV formation in multiple probands. Alu retrotransposons are nearly ubiquitous at 17p13.1 breakpoints, which is highly suggestive of Alu-mediated NAHR.[32] Alus make up the largest family of mobile elements in the human genome and have been implicated in a number of diseases, such as neurofibromatosis and breast cancer.[33,34] A large proportion of *MLH1* (chromosome 3p22.2) and *MSH2* (chromosome 2p21) deletions, which predispose one to Lynch syndrome, are mediated by Alu elements present at both breakpoints (24% and 85%, respectively, in one analysis),[35] whereas other non-Alu-mediated events are associated with the remaining breakpoints. Somatically acquired rearrangements are common in cancer, and it has been shown that regions with high levels of Alus are more susceptible to recombination in tumors.[32,36] Disruptions of *TP53*, by somatic mutation or loss of heterozygosity, are a virtual prerequisite for transformation of incipient cancer cells. Although the breakpoint resolution achieved in our study has yet to be examined in many cancer samples, at least one report has demonstrated that Alus can indeed mediate somatic rearrangements at *TP53*.[37] Future studies of cancer[38] will determine whether Alu-mediated recombination at 17p13.1 is as widespread in tumors as we show them to be in the germline.

This report adds 17p13.1 deletions—which result in two seemingly distinct phenotypes—to the list of disease loci associated with Alus. As more CNV-associated disorders are discovered, it will be intriguing to consider whether other loci in the genome also give rise to phenotypically distinct disorders by means of a common mechanism.

All cancer-associated *TP53* deletions reported to date are, to our knowledge, small (< 50 Kb)[39–41] and, except for one particularly complex Alu-mediated 45 Kb rearrangement,[40] involve only partial deletion of the gene. Whereas the cancer-specific susceptibility of LFS is well recognized, we show that 17p13.1 deletions are associated with a contiguous deletion syndrome involving a recognizable phenotype with DD, hypotonia, and hand and foot abnormalities. Furthermore, we demonstrate that a high-resolution array platform improves detection of previously unrecognized microdeletions, suggesting that it could provide a valuable tool in the molecular diagnosis of *TP53* wild-type LFS and for patients with cognitive-delay phenotypes.

Supplemental Data

Supplemental Data include four figures and two tables and can be found with this article online at http://www.cell.com/AJHG/.

Acknowledgments

Thanks to members of the Malkin Lab for assistance and proofreading and to Stephen Meyn, Stephen Scherer, Christian Marshall, and Dalila Pinto for critical review of the manuscript and discussion. Thanks also to Megan Kowalski for help with sample coordination and pedigree ascertainment and to the Cytogenomics Laboratory at the Children's Hospital of Philadelphia. The Centre for Applied Genomics (Toronto, Canada) is acknowledged for technical support. The research was supported by grants from the Canadian Cancer Society Research Institute (with funds from the Canadian Cancer Society), the Canadian Institutes for Health Research (D.M.), the SickKids Foundation, Canada Foundation for Innovation (D.M), and the Grundy Vision for Life fund (K.E.N.). A.S. is supported by a Canadian Institutes of Health Research Frederick Banting & Charles H. Best Doctoral Studentship Award.

Received: July 8, 2010
Revised: September 24, 2010
Accepted: October 12, 2010
Published online: November 4, 2010

Web Resources

The URLs for data presented herein are as follows:

Online Mendelian Inheritance in Man (OMIM), http://www.ncbi.nlm.nih.gov/Omim/

The International Agency for Research on Cancer (IARC) TP53 Mutation Database, http://www-p53.iarc.fr/

References

1. Stefansson, H., Rujescu, D., Cichon, S., Pietiläinen, O.P., Ingason, A., Steinberg, S., Fossdal, R., Sigurdsson, E., Sigmundsson, T., Buizer-Voskamp, J.E., et al; GROUP. (2008). Large recurrent microdeletions associated with schizophrenia. Nature *455*, 232–236.
2. International Schizophrenia Consortium. (2008). Rare chromosomal deletions and duplications increase risk of schizophrenia. Nature *455*, 237–241.
3. Greenway, S.C., Pereira, A.C., Lin, J.C., DePalma, S.R., Israel, S.J., Mesquita, S.M., Ergul, E., Conta, J.H., Korn, J.M., McCarroll, S.A., et al. (2009). De novo copy number variants identify new genes and loci in isolated sporadic tetralogy of Fallot. Nat. Genet. *41*, 931–935.
4. Diskin, S.J., Hou, C., Glessner, J.T., Attiyeh, E.F., Laudenslager, M., Bosse, K., Cole, K., Mossé, Y.P., Wood, A., Lynch, J.E., et al. (2009). Copy number variation at 1q21.1 associated with neuroblastoma. Nature *459*, 987–991.
5. Mefford, H.C., Sharp, A.J., Baker, C., Itsara, A., Jiang, Z., Buysse, K., Huang, S., Maloney, V.K., Crolla, J.A., Baralle, D., et al. (2008). Recurrent rearrangements of chromosome 1q21.1 and variable pediatric phenotypes. N. Engl. J. Med. *359*, 1685–1699.
6. Conrad, D.F., Pinto, D., Redon, R., Feuk, L., Gokcumen, O., Zhang, Y., Aerts, J., Andrews, T.D., Barnes, C., Campbell, P., et al. (2009). Origins and functional impact of copy number variation in the human genome. Nature *464*, 704–712.
7. Nagy, R., Sweet, K., and Eng, C. (2004). Highly penetrant hereditary cancer syndromes. Oncogene *23*, 6445–6470.
8. Shlien, A., Tabori, U., Marshall, C.R., Pienkowska, M., Feuk, L., Novokmet, A., Nanda, S., Druker, H., Scherer, S.W., and Malkin, D. (2008). Excessive genomic DNA copy number variation in the Li-Fraumeni cancer predisposition syndrome. Proc. Natl. Acad. Sci. USA *105*, 11264–11269.
9. Shlien, A., and Malkin, D. (2009). Copy number variations and cancer. Genome Med *1*, 62.
10. Malkin, D., Li, F.P., Strong, L.C., Fraumeni, J.F., Jr., Nelson, C.E., Kim, D.H., Kassel, J., Gryka, M.A., Bischoff, F.Z., Tainsky, M.A., et al. (1990). Germ line p53 mutations in a familial syndrome of breast cancer, sarcomas, and other neoplasms. Science *250*, 1233–1238.
11. Bayani, J., and Squire, J.A. (2004). Fluorescence in situ Hybridization (FISH). Curr Protoc. Cell. Biol., Chapter 22, Unit 22.24.
12. Malinge, S., Izraeli, S., and Crispino, J.D. (2009). Insights into the manifestations, outcomes, and mechanisms of leukemogenesis in Down syndrome. Blood *113*, 2619–2628.
13. Scherer, S.W., Lee, C., Birney, E., Altshuler, D.M., Eichler, E.E., Carter, N.P., Hurles, M.E., and Feuk, L. (2007). Challenges and standards in integrating surveys of structural variation. Nat. Genet. ***39*** (7, Suppl), S7–S15.
14. Kidd, J.M., Cooper, G.M., Donahue, W.F., Hayden, H.S., Sampas, N., Graves, T., Hansen, N., Teague, B., Alkan, C., Antonacci, F., et al. (2008). Mapping and sequencing of structural variation from eight human genomes. Nature *453*, 56–64.
15. Conrad, D.F., Bird, C., Blackburne, B., Lindsay, S., Mamanova, L., Lee, C., Turner, D.J., and Hurles, M.E. (2010). Mutation spectrum revealed by breakpoint sequencing of human germline CNVs. Nat. Genet. *42*, 385–391.
16. Perry, G.H., Ben-Dor, A., Tsalenko, A., Sampas, N., Rodriguez-Revenga, L., Tran, C.W., Scheffer, A., Steinfeld, I., Tsang, P., Yamada, N.A., et al. (2008). The fine-scale and complex architecture of human copy-number variation. Am. J. Hum. Genet. *82*, 685–695.
17. Lieber, M.R., Ma, Y., Pannicke, U., and Schwarz, K. (2003). Mechanism and regulation of human non-homologous DNA end-joining. Nat. Rev. Mol. Cell Biol. *4*, 712–720.
18. Kranz, C., Denecke, J., Lehrman, M.A., Ray, S., Kienz, P., Kreissel, G., Sagi, D., Peter-Katalinic, J., Freeze, H.H., Schmid, T., et al. (2001). A mutation in the human MPDU1 gene causes congenital disorder of glycosylation type If (CDG-If). J. Clin. Invest. *108*, 1613–1619.
19. Darnell, J.C., Fraser, C.E., Mostovetsky, O., and Darnell, R.B. (2009). Discrimination of common and unique RNA-binding activities among Fragile X mental retardation protein paralogs. Hum. Mol. Genet. *18*, 3164–3177.
20. Kullander, K., Butt, S.J., Lebret, J.M., Lundfald, L., Restrepo, C.E., Rydström, A., Klein, R., and Kiehn, O. (2003). Role of EphA4 and EphrinB3 in local neuronal circuits that control walking. Science *299*, 1889–1892.
21. Chompret, A., Brugières, L., Ronsin, M., Gardes, M., Dessarps-Freichey, F., Abel, A., Hua, D., Ligot, L., Dondon, M.G., Bressac-de Paillerets, B., et al. (2000). P53 germline mutations in childhood cancers and cancer risk for carrier individuals. Br. J. Cancer *82*, 1932–1937.
22. Schluth-Bolard, C., Sanlaville, D., Labalme, A., Till, M., Morin, I., Touraine, R., and Edery, P. (2010). 17p13.1 microdeletion involving the TP53 gene in a boy presenting with mental retardation but no tumor. Am. J. Med. Genet. A. *152A*, 1278–1282.
23. Adam, M.P., Justice, A.N., Schelley, S., Kwan, A., Hudgins, L., and Martin, C.L. (2009). Clinical utility of array comparative genomic hybridization: uncovering tumor susceptibility in individuals with developmental delay. J. Pediatr. *154*, 143–146.
24. Krepischi-Santos, A.C., Rajan, D., Temple, I.K., Shrubb, V., Crolla, J.A., Huang, S., Beal, S., Otto, P.A., Carter, N.P., Vianna-Morgante, A.M., and Rosenberg, C. (2009). Constitutional haploinsufficiency of tumor suppressor genes in mentally retarded patients with microdeletions in 17p13.1. Cytogenet. Genome Res. *125*, 1–7.
25. Schwarzbraun, T., Obenauf, A.C., Langmann, A., Gruber-Sedlmayr, U., Wagner, K., Speicher, M.R., and Kroisel, P.M. (2009). Predictive diagnosis of the cancer prone Li-Fraumeni syndrome by accident: new challenges through whole genome array testing. J. Med. Genet. *46*, 341–344.
26. Mahmoudi, S., Henriksson, S., Corcoran, M., Méndez-Vidal, C., Wiman, K.G., and Farnebo, M. (2009). Wrap53, a natural p53 antisense transcript required for p53 induction upon DNA damage. Mol. Cell *33*, 462–471.
27. Brosh, R., and Rotter, V. (2009). When mutants gain new powers: news from the mutant p53 field. Nat. Rev. Cancer *9*, 701–713.
28. de Vries, A., Flores, E.R., Miranda, B., Hsieh, H.M., van Oostrom, C.T., Sage, J., and Jacks, T. (2002). Targeted point mutations of p53 lead to dominant-negative inhibition of wild-type p53 function. Proc. Natl. Acad. Sci. USA *99*, 2948–2953.
29. Hainaut, P., and Wiman, K.G. (2009). 30 years and a long way into p53 research. Lancet Oncol. *10*, 913–919.
30. Mosner, J., Mummenbrauer, T., Bauer, C., Sczakiel, G., Grosse, F., and Deppert, W. (1995). Negative feedback regulation of wild-type p53 biosynthesis. EMBO J. *14*, 4442–4449.

31. Vilborg, A., Wilhelm, M.T., and Wiman, K.G. (2010). Regulation of tumor suppressor p53 at the RNA level. J. Mol. Med. *88*, 645–652.
32. Sen, S.K., Han, K., Wang, J., Lee, J., Wang, H., Callinan, P.A., Dyer, M., Cordaux, R., Liang, P., and Batzer, M.A. (2006). Human genomic deletions mediated by recombination between Alu elements. Am. J. Hum. Genet. *79*, 41–53.
33. Batzer, M.A., and Deininger, P.L. (2002). Alu repeats and human genomic diversity. Nat. Rev. Genet. *3*, 370–379.
34. Deininger, P.L., and Batzer, M.A. (1999). Alu repeats and human disease. Mol. Genet. Metab. *67*, 183–193.
35. Li, L., McVety, S., Younan, R., Liang, P., Du Sart, D., Gordon, P.H., Hutter, P., Hogervorst, F.B., Chong, G., and Foulkes, W.D. (2006). Distinct patterns of germ-line deletions in MLH1 and MSH2: the implication of Alu repetitive element in the genetic etiology of Lynch syndrome (HNPCC). Hum. Mutat. *27*, 388.
36. Smith, T.M., Lee, M.K., Szabo, C.I., Jerome, N., McEuen, M., Taylor, M., Hood, L., and King, M.C. (1996). Complete genomic sequence and analysis of 117 kb of human DNA containing the gene BRCA1. Genome Res. *6*, 1029–1049.
37. Slebos, R.J., Resnick, M.A., and Taylor, J.A. (1998). Inactivation of the p53 tumor suppressor gene via a novel Alu rearrangement. Cancer Res. *58*, 5333–5336.
38. Hudson, T.J., Anderson, W., Artez, A., Barker, A.D., Bell, C., Bernabé, R.R., Bhan, M.K., Calvo, F., Eerola, I., Gerhard, D.S., et al; International Cancer Genome Consortium. (2010). International network of cancer genome projects. Nature *464*, 993–998.
39. Bougeard, G., Sesboüé, R., Baert-Desurmont, S., Vasseur, S., Martin, C., Tinat, J., Brugières, L., Chompret, A., de Paillerets, B.B., Stoppa-Lyonnet, D., et al; French LFS working group. (2008). Molecular basis of the Li-Fraumeni syndrome: an update from the French LFS families. J. Med. Genet. *45*, 535–538.
40. Bougeard, G., Brugières, L., Chompret, A., Gesta, P., Charbonnier, F., Valent, A., Martin, C., Raux, G., Feunteun, J., Bressac-de Paillerets, B., and Frébourg, T. (2003). Screening for TP53 rearrangements in families with the Li-Fraumeni syndrome reveals a complete deletion of the TP53 gene. Oncogene *22*, 840–846.
41. Plummer, S.J., Santibáñez-Koref, M., Kurosaki, T., Liao, S., Noble, B., Fain, P.R., Anton-Culver, H., and Casey, G. (1994). A germline 2.35 kb deletion of p53 genomic DNA creating a specific loss of the oligomerization domain inherited in a Li-Fraumeni syndrome family. Oncogene *9*, 3273–3280.
42. Knudson, A.G., Jr. (1971). Mutation and cancer: statistical study of retinoblastoma. Proc. Natl. Acad. Sci. USA *68*, 820–823.